

Structural basis for inhibition of DNA replication by aphidicolin

Andrey G. Baranovskiy¹, Nigar D. Babayeva¹, Yoshiaki Suwa¹, Jianyou Gu¹, Youri I. Pavlov^{1,2,3} and Tahir H. Tahirov^{1,*}

¹Eppley Institute for Research in Cancer and Allied Diseases, University of Nebraska Medical Center, Omaha, NE 68198, USA, ²Department of Biochemistry and Molecular Biology, University of Nebraska Medical Center, Omaha, NE 68198, USA and ³Department of Pathology and Microbiology, University of Nebraska Medical Center, Omaha, NE 68198, USA

Received August 01, 2014; Revised October 10, 2014; Accepted November 05, 2014

ABSTRACT

Natural tetracyclic diterpenoid aphidicolin is a potent and specific inhibitor of B-family DNA polymerases, haltering replication and possessing a strong antimitotic activity in human cancer cell lines. Clinical trials revealed limitations of aphidicolin as an antitumor drug because of its low solubility and fast clearance from human plasma. The absence of structural information hampered the improvement of aphidicolin-like inhibitors: more than 50 modifications have been generated so far, but all have lost the inhibitory and antitumor properties. Here we report the crystal structure of the catalytic core of human DNA polymerase α (Pol α) in the ternary complex with an RNA-primed DNA template and aphidicolin. The inhibitor blocks binding of dCTP by docking at the Pol α active site and by rotating the template guanine. The structure provides a plausible mechanism for the selectivity of aphidicolin incorporation opposite template guanine and explains why previous modifications of aphidicolin failed to improve its affinity for Pol α . With new structural information, aphidicolin becomes an attractive lead compound for the design of novel derivatives with enhanced inhibitory properties for B-family DNA polymerases.

INTRODUCTION

Genome replication in eukaryotes relies on DNA polymerases of the B-family, comprising Pol α , Pol δ , Pol ϵ and Pol ζ . Pol α in a tight complex with primase plays an essential role in initiation of replication by synthesizing primers for major replicative DNA polymerases δ and ϵ (1,2). The large catalytic subunit of Pol α (p180 in humans) possesses the 3'-directed DNA-polymerizing activity and together with the smaller B-subunit mediates interactions with pri-

mase and other components of the replicative apparatus (3–8). The structures of the orthologous yeast Pol α DNA-polymerizing domain in apo-form, in binary complex with DNA, and in ternary complex with DNA and dGTP, have been recently reported (7). Organization of the catalytic domain is similar to B-family DNA-polymerases (9,10) and their prototypes from viruses, bacteriophages and bacteria (11–13). It adopts the universal ‘right-hand’ DNA polymerase fold with an active site formed by a ‘palm’ holding the catalytic residues, a ‘thumb’ that binds the primer-template duplex and ‘fingers’ interacting with incoming nucleotide.

The tetracyclic diterpenoid aphidicolin, an antimitotic and antiviral metabolite of the mold *Cephalosporium aphidicola*, is a potent inhibitor of DNA replication in a variety of organisms (14–17). It specifically inhibits B-family DNA polymerases from eukaryotes (18–21), bacteria (22) and viruses (15,23–25). Despite the absence of structural homology between aphidicolin and dNTPs, the drug binds at or near the nucleotide-binding site (14,26). There is some variation in the effects of aphidicolin on different DNA polymerases. For example, aphidicolin inhibits incorporation of dCTP by Pol α more effectively in comparison to other dNTPs, while such selectivity is not seen for Pol ϵ (19,26).

In contrast to nucleotide analogues that usually have an inhibitory effect on multiple metabolic pathways, aphidicolin does not affect DNA methylation or RNA, protein and nucleotide biosynthesis. Because of its specificity and reversibility, aphidicolin was successfully employed for synchronization of mammalian cell cultures (23,27–29). The addition of aphidicolin results in cell cycle pause at the G1/S border. In cells that have already entered S phase, the DNA synthesis stops, while nondividing cells are not affected by the drug (17,30). Aphidicolin demonstrated potent growth-inhibitory and cytotoxic activities against human tumor cell lines cultured *in vitro* (31,32). Aphidicolin’s potential in the treatment of cancer was explored in clinical trials by the Eu-

*To whom correspondence should be addressed. Tel: +1 402 559 7607; Fax: +1 402 559 3739; Email: ttahirov@unmc.edu

ropean Organization for Research and Treatment of Cancer (33). These studies revealed the limitations of aphidicolin as antitumor drug due to low solubility and fast clearance from human plasma because of degradation in the liver by cytochrome P-450 (34). More than 50 aphidicolin modifications have been generated so far to increase solubility, but all of them negatively affected its inhibitory properties (25,35,36). The lack of structural information has hampered the successful design of aphidicolin modifications to improve inhibitory properties while overcoming the solubility problem.

Here we report the crystal structure of the catalytic core of human Pol α in ternary complex with an RNA-primed DNA template and aphidicolin. The structure explains the mechanism of aphidicolin's inhibitory effect, and will serve as a model for design of highly efficient inhibitors of DNA replication and anticancer drugs. This is the first reported structure of the human Pol α catalytic core as well as the inhibitory complex of eukaryotic replicative DNA polymerase.

MATERIALS AND METHODS

Reagents

Aphidicolin was obtained from the Acros Organics. Reagents used for crystallization were obtained from Hampton Research. All other reagents were from Fisher Scientific.

Oligonucleotides

Oligonucleotides used for crystallization were obtained from IDT Inc. DNA template—5'-ATTACTATAGGCGCTCCAGGC; RNA primer—5'-rGrCrCrUrGrArGrCrG/ddC/ (/ddC/ is a dideoxycytidine). The DNA/RNA duplex was obtained at 0.2 mM concentration by annealing at 43°C for 30 min (after heating at 70°C for 1 min) in buffer containing 10 mM Tris-HCl, pH 7.9, 70 mM KCl.

Cloning, expression and purification

Cloning, expression and purification of the catalytic core of human Pol α has been recently described (37). Briefly, the gene fragment corresponding to p180 residues 335–1257 was cloned to pFastBac1 transfer vector (Life Technologies), which contained the DNA sequence coding for the N-terminal His-tag followed by the TEV protease recognition site. The obtaining of high-titer baculoviruses and protein expression in Sf21 insect cells was completed according to manufacturer's instructions. The Pol α catalytic core with cleavable N-terminal His₆-tag was purified to near homogeneity (Supplementary Figure S1A) in four steps including chromatography on Ni-IDA column (Bio-Rad), His-tag digestion by TEV protease during dialysis, pass through Ni-IDA column and chromatography on Heparin HP HiTrap column (GE Healthcare) (37). Peak fractions were dialyzed to 10 mM Tris-HCl, pH 7.7, 0.1 M KCl, 1% glycerol, 1 mM DTT. Dialyzed protein sample (1 ml; 15 μ M Pol α ; 1.6 mg/ml) was mixed with 0.5 ml of dialysis buffer containing 36 μ M RNA-primed DNA template, 3.6 mM MgCl₂ and

60 μ M aphidicolin, which was added from 15 mM stock in dimethyl sulfoxide. The obtained ternary complex was concentrated 10-fold and flash frozen in liquid nitrogen.

Crystallization

The diffraction-quality crystals (Supplementary Figure S1B) were obtained at 295 K in 100 mM KCl, 12.5 mM MgCl₂, 25 mM Na-cacodylate, pH 6.5, 6% 2-propanol, 2 mM tris(2-carboxyethyl)phosphine. All the crystals were soaked in cryoprotectant solution for a few seconds, scooped in a nylon-fiber loop and flash cooled in a dry nitrogen stream at 100 K. The cryoprotectant solution contained 100 mM KCl, 10 mM MgCl₂, 25 mM Na-cacodylate, pH 6.5, 5.6% 2-propanol, 10% polyethylene glycol 200, 10% ethylene glycol. All initial diffraction data were obtained on a Rigaku R-AXIS IV imaging plate using Osmic VariMaxTM HR mirror-focused CuK α radiation from a Rigaku FR-E rotating anode operated at 45 kV and 45 mA. Complete diffraction datasets were collected using synchrotron X-rays on the Argonne National Laboratory (ANL) Advanced Photon Source (APS) beamline 24-ID-E using ADSC Quantum 315 detector. All intensity data were indexed, integrated and scaled with DENZO and SCALEPACK from the HKL-2000 program package (38).

Structure determination

The Pol α -DNA/RNA-aphidicolin complex was crystallized in the orthorhombic $P2_12_12_1$ space group, with two copies of the ternary complex in the asymmetric unit. The structure was determined by the molecular replacement method using the coordinates of the human Pol α -DNA/RNA-dCTP complex (PDB id 4QCL). The electron density for the fingers domain revealed large differences, so the entire fingers domain was removed from each molecule and rebuilt again. The initial structure was refined without aphidicolin and then locations of aphidicolin and their conformations were determined from a difference $F_o - F_c$ Fourier map. Then the aphidicolin and water molecules were added to the model and refined. The final model has an excellent geometry with 88.6% of residues located in the core and 11.2% in the allowed regions of the Ramachandran plot. The structured regions in both molecules started with Glu338 and ended with Thr1244, thus containing all conservative domains of the Pol α catalytic core (7). Amino acid residues 809–833 and 883–895 were not visible or were poorly ordered in the electron density maps, and therefore were excluded from the final model. In addition, molecule B has a small unstructured four-residue region between Leu673 and Gly678. Structure determination and refinement were performed using CNS software (39). Model building was performed with the Turbo-Frodo software. Final refinement statistics are provided in Supplementary Table S1.

Miscellaneous

Figure 1 was prepared with the Turbo-Frodo software, and Supplementary Figure S2 with the LigPlot⁺ v.1.5. All other figures were prepared with the PyMOL Molecular Graphics

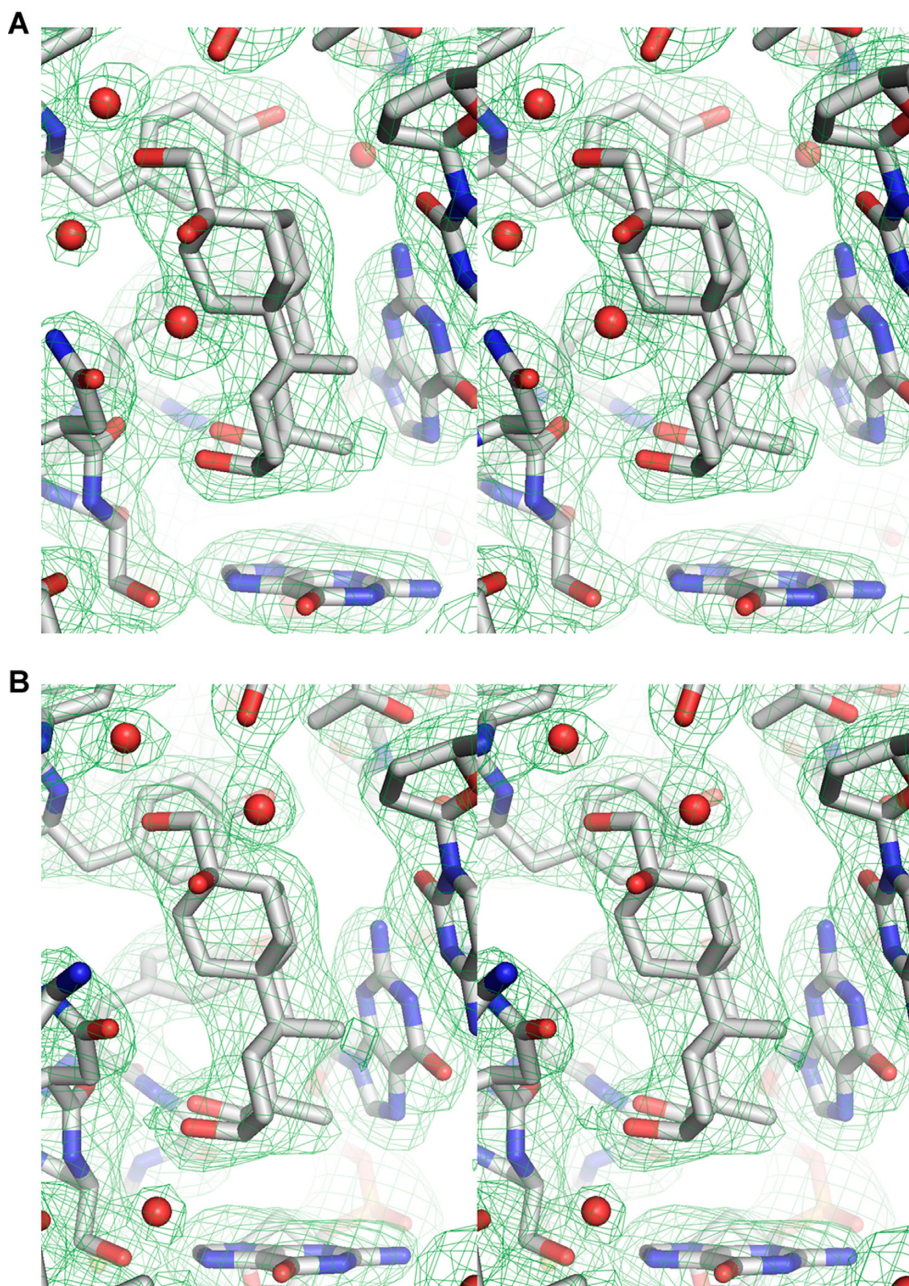


Figure 1. The electron density maps. The $2F_0 - F_c$ Fourier maps covering aphidicolin and surrounding residues in the first (**A**) and in the second (**B**) independent molecules are displayed at contour level of 1.0σ . Aphidicolin and protein are drawn as sticks, the water molecules are drawn as balls and the electron density maps are drawn as mesh.

System, Version 1.7.0.5, Schrödinger, LLC. Modeling was performed by using the ‘Editing’ mode of the PyMOL software. At the final step of aphidicolin derivatives modeling, the Merck Molecular Force Field (MMFF) was applied to perform the energy minimization.

RESULTS

Overall structure of the Pol α -DNA/RNA-aphidicolin complex

We crystallized the catalytic core of human Pol α in a ternary complex with an RNA-primed DNA template and aphidicolin (Pol α -DNA/RNA-aphidicolin), and determined the crystal structure at 2.5 \AA resolution. The crystal contains two nearly identical molecules in the asymmetric unit with a root mean square deviation (rmsd) of 803 α -carbon atoms of 0.11 \AA . The difference Fourier map of

the initially refined complex without aphidicolin revealed the well-defined structure of aphidicolin with all three of its six-membered rings acquiring chair conformation (Figure 1). Consistent with previously accumulated biochemical data, aphidicolin docks at the dCTP-binding site opposite template guanine (Figures 2 and 3) and does not affect Pol α interaction with primed template (17,26,40). Unlike flat nitrogenous bases, aphidicolin has an elongated bulky ‘potato’ shape and occupies a space in the active site that is designated for the base and sugar of incoming dNTP and the pairing base of the template nucleotide but not the triphosphate moiety of dNTP.

Aphidicolin interaction with Pol α

Despite the absence of structural similarity between aphidicolin and the nucleotides, aphidicolin fits well into the hydrophobic pocket formed by the terminal G:C base pair, with the ribose of the RNA primer, the template guanine and several residues of Pol α including Tyr865, Tyr957, Leu864, Asn954, Ser955 and Gly958 (Figures 2B and 4A). The water-mediated contacts between Pol α and aphidicolin are different in the two independent molecules (Supplementary Figure S2) and, probably, do not play a significant role in aphidicolin binding. Notably, all four hydroxyls of aphidicolin are located on one side of molecule, which is opposite to the planar G:C base pair. Two of these hydroxyls form the hydrogen bonds with the main-chain atoms of the fingers and palm domains: O17 interacts with a nitrogen of Tyr865 (2.9 Å) and O18 interacts with an oxygen of Asn954 (2.8 Å) and the nitrogen of Gly958 (3.1 Å) (Figures 2C and 4A).

Alignment with a ternary complex containing dCTP instead of aphidicolin (PDB code 4QCL) demonstrated high conformational similarity between the Pol α catalytic core domains in both complexes (rmsd is 1.0 Å for 781 C α), except for substantial difference in the active site and the conformation of the fingers (Figure 3). In contrast to the typical closed conformation of B-family DNA polymerase ternary complexes with incoming dNTP (7,9–11), the fingers in the complex with aphidicolin adopted an open conformation like in yeast Pol α without bound dNTP (Supplementary Figure S3). This is due to the lack of triphosphate moiety in aphidicolin that is necessary to form the hydrogen bonds with the fingers and move them toward the palm domain. Comparison with the yeast Pol α -DNA/RNA (PDB code 4FXD) (7) shows that interaction of aphidicolin with a main-chain nitrogen of Gly958 shifts the finger residues Met956-Gly961, reducing the distance between Asn954 O and Gly958 N from 5.7 to 3.8 Å. As a result, the second helix of fingers is straighter in aphidicolin-bound complex (Figure 4B and Supplementary Figure S4A). We suggest that human Pol α in open conformation (without aphidicolin) should have the same helix disruption like the yeast analog because both enzymes have very similar conformation of that region in the closed conformation (Supplementary Figure S4B). Moreover, the same or similar disruption was observed in apo-forms of yeast Pol α and Pol α -like DNA-polymerases from other organisms (Supplementary Figure S5A) (7,12,13,41). Such helix distortion is specific to the open conformation because it is not observed in the closed

forms of the yeast and human Pol α (Supplementary Figure S4B) and other B-family DNA polymerases (Supplementary Figure S5B) (9–12).

Aphidicolin displaces the template guanine from the Pol α active site

In addition to local changes in protein structure, aphidicolin binding also introduces dramatic changes in the position of unpaired template guanine due to sterical hindrance with an A-ring of aphidicolin: the base is rotated clockwise around the glycosidic bond by 118° (Figure 3B) and fits into the pocket formed by the side chains of Arg784, Ser955 and Cys959, by main chains of Ser955, Gly958 and Cys959, and aphidicolin A-ring with 3,18-OH groups (Figure 5A). Additionally, the hydrogen bond between N7 of guanine and Oy of Ser 955 stabilizes the guanine in that pocket. It is interesting to note, that the same region of the helix (954–958) interacts with aphidicolin and template guanine.

The intriguing feature of aphidicolin to inhibit Pol α more efficiently when it binds opposite template guanine is finally explained here. According to biochemical data, aphidicolin most efficiently inhibits incorporation of dCTP ($K_i \sim 0.2 \mu\text{M}$ for calf thymus Pol α), followed by dTTP (26,40). It inhibits the incorporation of dGTP and dATP 10-fold less efficiently. The modeling of cytosine instead of guanine reveals a sterical clash with Ser955 (2.4 Å between C5 and Oy, respectively; Figure 5B). Rotation of cytosine around the glycosidic bond will cause sterical hindrance with the side chains of Ser955 and/or Arg784, or the A-ring of aphidicolin. Thymine has a methyl group at C5 that would result in higher degree of sterical hindrance compared to cytosine. The main difference between adenine and guanine is the replacement of an O6 keto-group, which gets a negative charge in one of two tautomeric forms, by an NH₂ group, which is protonated at physiological conditions. Therefore, instead of weak electrostatic attraction with a guanidine group of Arg784, there is repulsion between the two positively charged groups. This may result in a less stable conformation of adenine affecting aphidicolin binding by Pol α .

Structure-based analysis of aphidicolin derivatives

Our structural data confirmed previous studies about the critical role of hydroxyls 17 and 18 in the interaction with Pol α . The removal or acetylation of 17-OH or 18-OH resulted in over a 10-fold reduction of aphidicolin inhibitory activity (Supplementary Table S2) (35,36,42). 3-oxo or 3-deoxy aphidicolin derivatives demonstrated moderate reduction of inhibitory properties, from 3- to 10-fold (36,42,43). Consistent with the low impact of 3-OH removal, this derivative does not form a critical hydrogen bond with protein. However, it forms a hydrogen bond with 18-OH that fixes the A-ring in a chair conformation and reduces the presence of stereoisomers with a boat conformation (Figure 2C). Inversion of 3 α - to 3 β -OH in aphidicolin resulted in complete loss of inhibitory activity (35,36,42). Modeling of 3 β -OH reveals that it makes a sterical hindrance with template guanine, so this derivative cannot fit the Pol α active site without its significant distortion (Figure 6A), thus explaining the loss of inhibition. The methyl

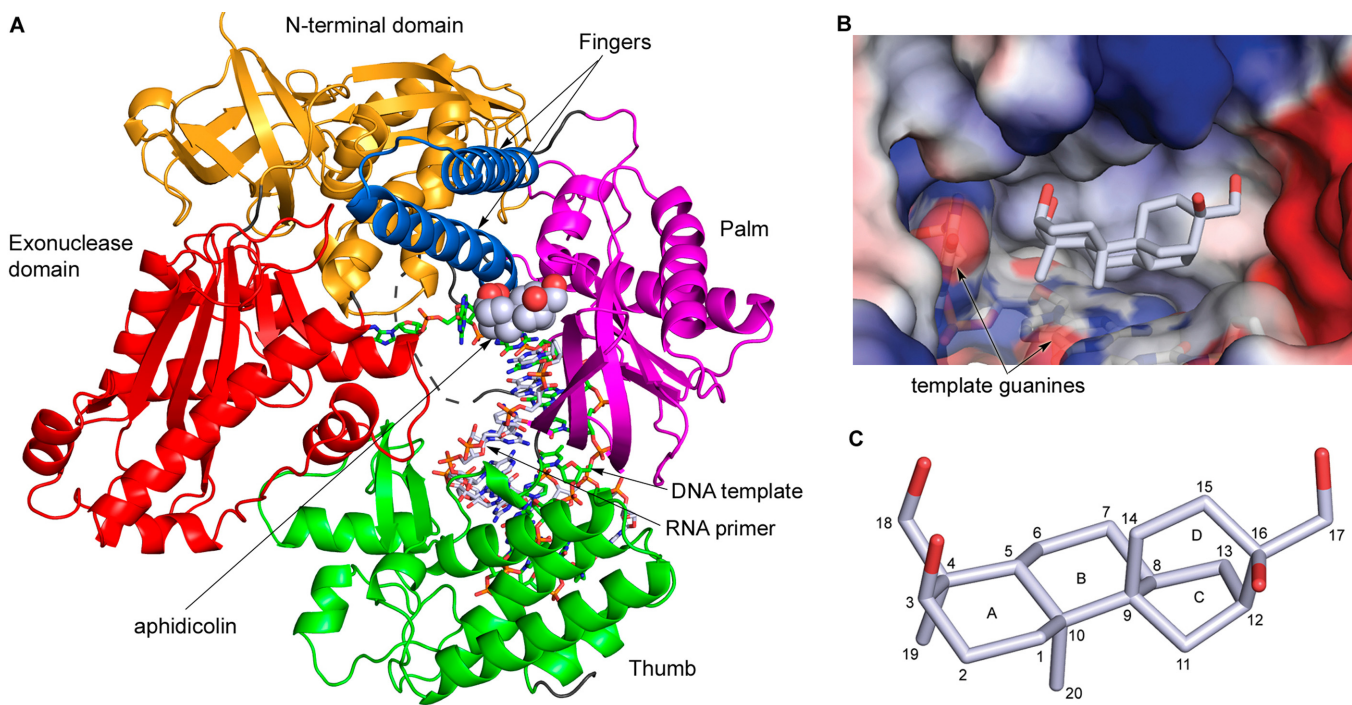


Figure 2. Structure of the human Pol α -DNA/RNA-aphidicolin ternary complex. (A) The overall view of the ternary complex. Protein is represented as cartoon, DNA/RNA as sticks and aphidicolin as spheres. The N-terminal domain is colored orange, the nonfunctional exonuclease domain—red, the palm—magenta, the fingers—marine, the thumb—lime-green and the linkers between domains—gray. The disordered linker between the N-terminal and palm domains is shown by dashed line. Aphidicolin atoms are colored gray for carbon and red for oxygen. DNA and RNA atoms are colored blue for nitrogen, red for oxygen, orange for phosphorus, and green or gray for DNA or RNA carbons, respectively. (B) Close-up view of the aphidicolin-binding pocket. Aphidicolin is shown as sticks. The protein surface is represented by the vacuum electrostatic potential; the DNA/RNA surface is shown at 50% transparency. (C) Structure of aphidicolin with numbered carbon positions.

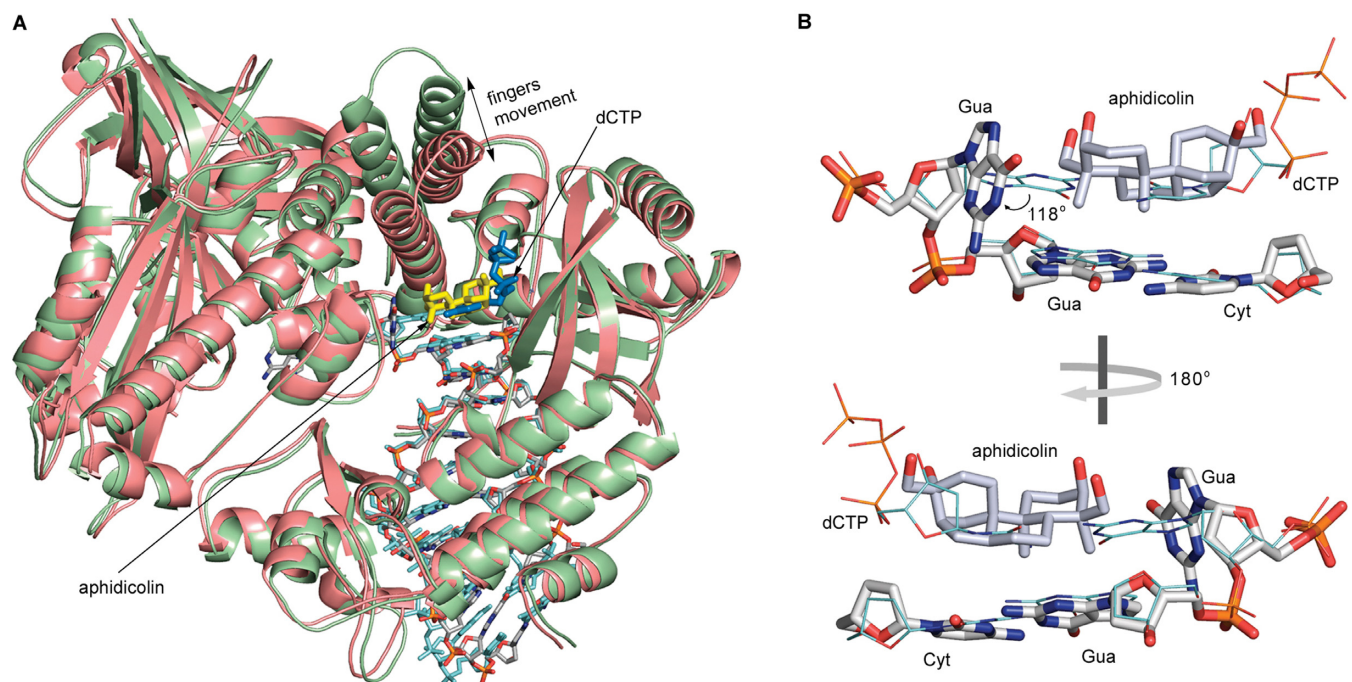


Figure 3. Alignment of human Pol α -DNA/RNA ternary complexes containing aphidicolin or dCTP. (A) The overall view of aligned ternary complexes. Proteins are represented as cartoon, all other molecules as sticks. For the complex with aphidicolin, the protein is colored pale-green, aphidicolin—yellow and DNA/RNA carbons—gray. For the complex containing dCTP, the protein is colored salmon, DNA/RNA—cyan and dCTP—marine. (B) Close-up view of aligned aphidicolin, dCTP and surrounding DNA/RNA bases. All atoms in aphidicolin complex are shown as sticks, and in dCTP complex as lines. For the ternary complexes containing aphidicolin or dCTP, the carbon atoms of DNA/RNA are colored gray or cyan, respectively.

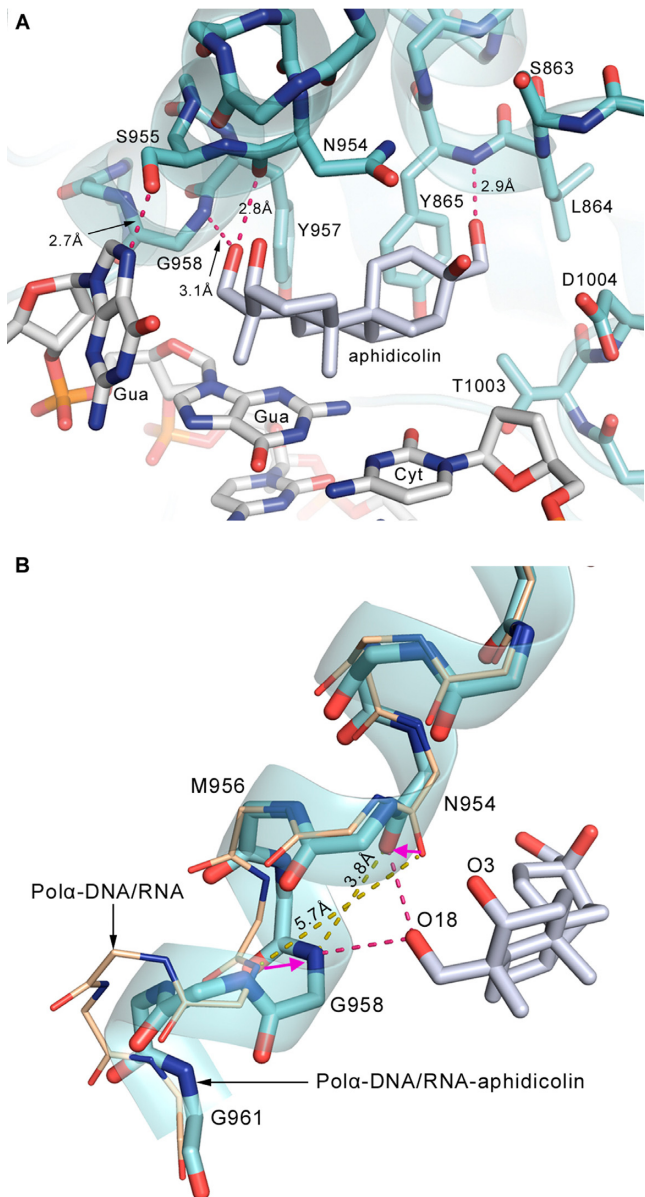


Figure 4. Interaction of aphidicolin with human Pol α . (A) Close-up view of aphidicolin in the active site of Pol α . Protein is represented as cartoon with 80% transparency; additionally, the main chain and residues located near aphidicolin are shown as sticks. DNA/RNA and aphidicolin are represented as sticks. Pol α atoms are colored blue for nitrogen, red for oxygen, yellow for sulfur and cyan for carbon. The predicted hydrogen bonds between aphidicolin, guanine and protein are shown by pink dashed lines. (B) Close-up view of the helix region interacting with aphidicolin after an alignment of the fingers domains from two complexes of Pol α in open conformation. For the human Pol α -DNA/RNA-aphidicolin complex, the main-chain atoms of the fingers domain are represented as sticks and colored cyan for carbon. Additionally, this finger helix is represented as cartoon with 80% transparency. For yeast Pol α -DNA/RNA complex (PDB code 4FXD (7)), the main-chain atoms of the fingers domain are represented as lines and colored wheat for carbon. Magenta arrows show the shift of N954 O and G958 N induced by aphidicolin binding.

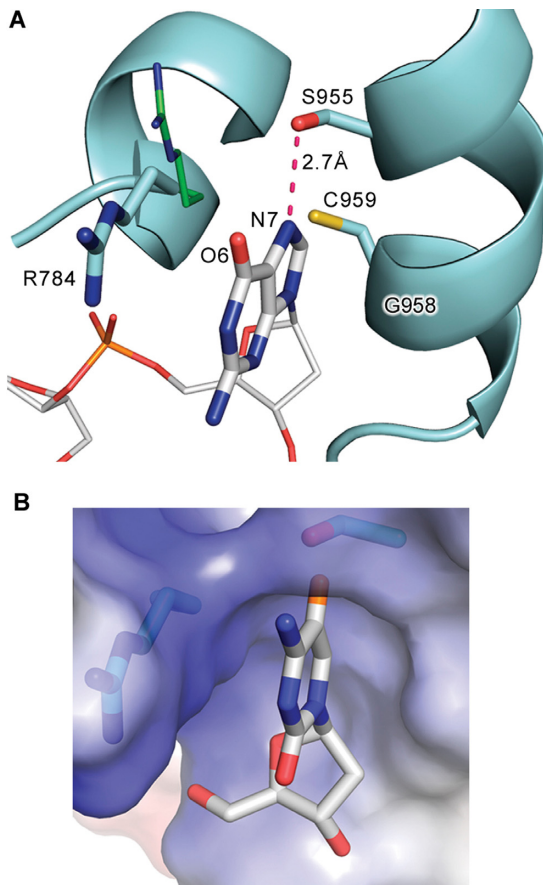


Figure 5. Mechanism of aphidicolin selectivity to template guanine. (A) The position of twisted guanine is stabilized by interaction with a side chain of Ser955. The color scheme for DNA/RNA and Pol α atoms is the same as on Figure 3A. Side-chain atoms of Arg784 from the ternary complex containing dCTP are colored blue for nitrogen and green for carbon. Aphidicolin atoms are omitted for clarity. (B) The modeled cytosine does not fit into the pocket due to sterical clash with Ser955. The hydrogen atom at C4 is shown and colored orange. Pol α surface is represented by the vacuum electrostatic potential. The modeling of cytosine in place of guanine was done with the PyMOL by keeping the position of the ribose and connected with it nitrogen from the nucleotide base unaltered.

or ethynyl groups in 3 β -position will also have a sterical clash with template guanine, thus explaining a profound decrease of their inhibitory activity (Supplementary Table S2). Other aphidicolin derivatives whose low activity is not connected with the deletion or modification of the critical hydroxyls 17-OH and 18-OH bear the next modifications: 2,3- α -epoxy, 2 α -methyl, 3 α -methyl and 2-ene-3-deoxy. The modeling analysis of 2,3- α -epoxy and 2-ene-3-deoxy derivatives demonstrates a change in the A-ring conformation, which affects the position of O18 (Supplementary Figure S6). The replacement of 3 α -OH with methyl would result in destabilization of the chair conformation of the A-ring and in sterical clash with the hydrophilic peptide bond between Asn954 and Ser955 (Supplementary Figure S6C). Severe defect of the inhibitory activity of 2 α -methyl aphidicolin is not obvious and could be explained by a change in the relative orientation of 3-OH and 18-OH, affecting the hydrogen bond between them and, therefore, the A-ring conformation.

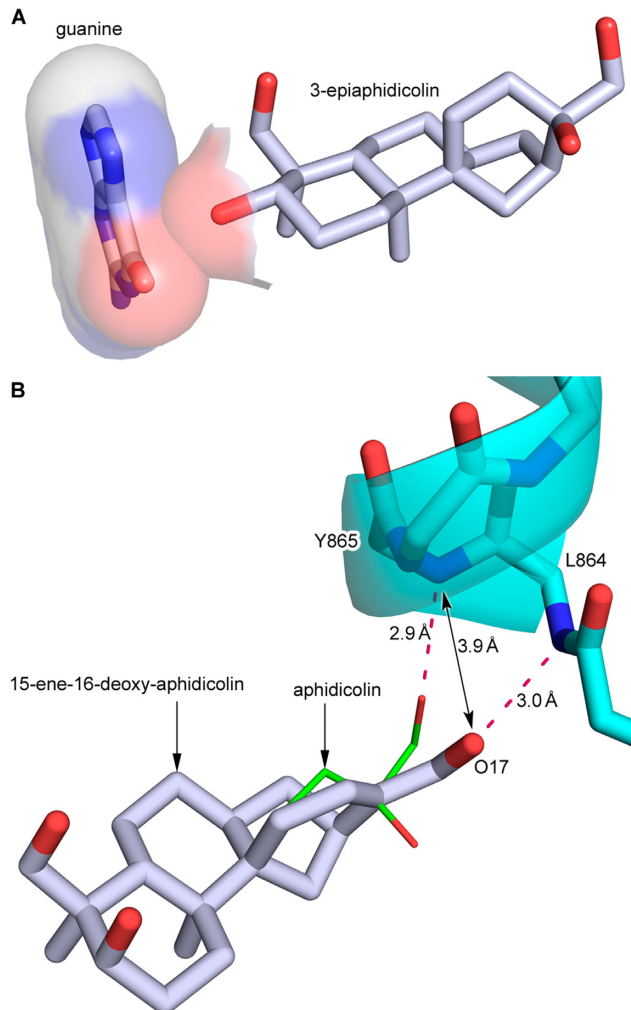


Figure 6. Modeling of aphidicolin derivatives. (A) Sterical hindrance between 3 β -OH of 3-epiaphidicolin and C6, O6 of template guanine. The surfaces of guanine and 3 β -OH are shown at 80% transparency. (B) Alignment of aphidicolin and its 15-ene-16-deoxy derivative. Pol α is represented as cartoon with 40% transparency. Aphidicolin is shown as lines; its derivative and the main-chain atoms of Pol α are shown as sticks. The carbons of aphidicolin, its derivative and Pol α are colored green, gray and cyan, respectively. The hydrogen bond between O17 of aphidicolin and Y865 N as well as the predicted hydrogen bond between O17 of 15-ene-16-deoxy-aphidicolin and Leu864 N are shown by red dashed lines.

The 16-OH group does not interact with Pol α (Figure 4A and Supplementary Figure S2) and has a significant potential for aphidicolin modifications improving its solubility and affinity. Curiously, the impact of this hydroxyl alone on aphidicolin properties has not been studied so far. All known modifications of O16 were combined with other changes in aphidicolin structure, which therefore masked the role of that oxygen (Supplementary Table S2) (25,35,42). For example, the inhibitory activity of 15-ene-16-deoxy-aphidicolin, where the 16-OH removal was combined with the generation of a double bond between carbons 15 and 16, was reduced only 3-fold. This reduction is probably due to the change in conformation of the D-ring and therefore in the position of 17-OH, affecting its interaction with Pol α (Figure 6B). In 16-oxo and 16-demethoxy derivatives, the

critical 17-OH is absent, which results in severe reduction of aphidicolin inhibitory properties.

DISCUSSION

Structural data provided here reveal that aphidicolin binds Pol α at the active site by occupying the hydrophobic pocket between the palm domain and the second helix of the fingers domain. Aphidicolin interaction with the base of that helix significantly changes its conformation resulting in minimization of the distortion characteristic to the open forms of DNA polymerases from the B-family. Moreover, the same region of the second helix also participates in formation of the pocket, which is ideally fitted by the imidazole ring of the template guanine displaced from the active site by aphidicolin.

The low solubility of aphidicolin is a major obstacle for its use as an antitumor drug (32,33,44,45) and numerous attempts to overcome this problem have failed. The structure of Pol α -DNA/RNA-aphidicolin complex explains the effects of known aphidicolin modifications on its inhibitory properties and provides a valuable rationale for design of a new generation of drugs with superior solubility, stability and inhibitory activity toward Pol α and other B-family DNA polymerases compared to aphidicolin. For example, O16 is located near the triphosphate-binding site (Figure 3B) and could be targeted for covalent coupling with di- or triphosphate (Supplementary Figure S7A). This modification can dramatically increase aphidicolin solubility and affinity for Pol α . Alternatively, O16 might be used for linking to specially designed compounds, which can target aphidicolin toward cancer cells. Interestingly, the C12 might be connected through the linker to the 2'-end of the primer strand (Supplementary Figure S7B). This may allow for selectively inhibiting the growth of tumor cells with cancer-associated unique sequences of genomic DNA, for example, in the case of translocations, deletions or regions of kataegis clustered mutations.

ACCESSION NUMBERS

The crystal structure coordinates of human Pol α in complex with DNA/RNA and aphidicolin have been deposited in PDB under accession number 4Q5V.

SUPPLEMENTARY DATA

Supplementary Data are available at NAR Online.

ACKNOWLEDGMENT

We thank S. Romanova for advice in aphidicolin chemistry, and J. Lovelace and G. E. Borgstahl for maintenance and management of the Eppley Institute's X-ray Crystallography Core Facility.

FUNDING

National Institute of General Medical Sciences (NIGMS) [GM101167 to T.H.T.]; National Cancer Institute (NCI)

[CA129925 to Y.I.P., in part]; NCI [P30CA036727 to Kenneth H. Cowan, in part]; NIGMS [P41 GM103403 to research conducted at the APS on the NECAT beamlines, in part]. Use of the APS, an Office of Science User Facility operated for the U.S. Department of Energy (DOE) Office of Science by ANL, was supported by the U.S. DOE under Contract No. DE-AC02-06CH11357. Funding for open access charge: NIGMS [GM101167].

Conflict of interest statement. None declared.

REFERENCES

- Garg,P. and Burgers,P.M. (2005) DNA polymerases that propagate the eukaryotic DNA replication fork. *Crit. Rev. Biochem. Mol. Biol.*, **40**, 115–128.
- Pavlov,Y.I. and Shcherbakova,P.V. (2010) DNA polymerases at the eukaryotic fork-20 years later. *Mutat. Res.*, **685**, 45–53.
- Mizuno,T., Yamagishi,K., Miyazawa,H. and Hanaoka,F. (1999) Molecular architecture of the mouse DNA polymerase alpha-primase complex. *Mol. Cell. Biol.*, **19**, 7886–7896.
- Kilkenny,M.L., De Piccoli,G., Perera,R.L., Labib,K. and Pellegrini,L. (2012) A conserved motif in the C-terminal tail of DNA polymerase alpha tethers primase to the eukaryotic replisome. *J. Biol. Chem.*, **287**, 23740–23747.
- Klinge,S., Nunez-Ramirez,R., Llorca,O. and Pellegrini,L. (2009) 3D architecture of DNA Pol alpha reveals the functional core of multi-subunit replicative polymerases. *EMBO J.*, **28**, 1978–1987.
- Huang,H., Weiner,B.E., Zhang,H., Fuller,B.E., Gao,Y., Wile,B.M., Zhao,K., Arnett,D.R., Chazin,W.J. and Fanning,E. (2010) Structure of a DNA polymerase alpha-primase domain that docks on the SV40 helicase and activates the viral primosome. *J. Biol. Chem.*, **285**, 17112–17122.
- Perera,R.L., Torella,R., Klinge,S., Kilkenny,M.L., Maman,J.D. and Pellegrini,L. (2013) Mechanism for priming DNA synthesis by yeast DNA polymerase alpha. *Elife*, **2**, e00482.
- Simon,A.C., Zhou,J.C., Perera,R.L., van Deursen,F., Evrin,C., Ivanova,M.E., Kilkenny,M.L., Renault,L., Kjaer,S., Matak-Vinkovic,D., Labib,K., Costa,A. and Pellegrini,L. (2014) A Ctf4 trimer couples the CMG helicase to DNA polymerase alpha in the eukaryotic replisome. *Nature*, **510**, 293–297.
- Hogg,M., Osterman,P., Bylund,G.O., Ganai,R.A., Lundstrom,E.B., Sauer-Eriksson,A.E. and Johansson,E. (2013) Structural basis for processive DNA synthesis by yeast DNA polymerase varepsilon. *Nat. Struct. Mol. Biol.*, **21**, 49–55.
- Swan,M.K., Johnson,R.E., Prakash,L., Prakash,S. and Aggarwal,A.K. (2009) Structural basis of high-fidelity DNA synthesis by yeast DNA polymerase delta. *Nat. Struct. Mol. Biol.*, **16**, 979–986.
- Franklin,M.C., Wang,J. and Steitz,T.A. (2001) Structure of the replicating complex of a pol alpha family DNA polymerase. *Cell*, **105**, 657–667.
- Wang,F. and Yang,W. (2009) Structural insight into translesion synthesis by DNA Pol II. *Cell*, **139**, 1279–1289.
- Liu,S., Knafoels,J.D., Chang,J.S., Waszak,G.A., Baldwin,E.T., Deibel,M.R. Jr, Thomsen,D.R., Homa,F.L., Wells,P.A., Tory,M.C. et al. (2006) Crystal structure of the herpes simplex virus 1 DNA polymerase. *J. Biol. Chem.*, **281**, 18193–18200.
- Brundret,K.M., Dalziel,W., Hesp,B., Jarvis,J.A.J. and Neidle,S. (1972) X-Ray crystallographic determination of the structure of the antibiotic aphidicolin: a tetracyclic diterpenoid containing a new ring system. *J. Chem. Soc. Chem. Commun.*, **18**, 1027–1028.
- Bucknall,R.A., Moores,H., Simms,R. and Hesp,B. (1973) Antiviral effects of aphidicolin, a new antibiotic produced by Cephalosporium aphidicola. *Antimicrob. Agents Chemother.*, **4**, 294–298.
- Huberman,J.A. (1981) New views of the biochemistry of eucaryotic DNA replication revealed by aphidicolin, an unusual inhibitor of DNA polymerase alpha. *Cell*, **23**, 647–648.
- Ikegami,S., Taguchi,T., Ohashi,M., Oguro,M., Nagano,H. and Mano,Y. (1978) Aphidicolin prevents mitotic cell division by interfering with the activity of DNA polymerase-alpha. *Nature*, **275**, 458–460.
- Byrnes,J.J. (1984) Structural and functional properties of DNA polymerase delta from rabbit bone marrow. *Mol. Cell. Biochem.*, **62**, 13–24.
- Cheng,C.H. and Kuchta,R.D. (1993) DNA polymerase epsilon: aphidicolin inhibition and the relationship between polymerase and exonuclease activity. *Biochemistry*, **32**, 8568–8574.
- Bambara,R.A. and Jesse,C.B. (1991) Properties of DNA polymerases delta and epsilon, and their roles in eukaryotic DNA replication. *Biochim. Biophys. Acta*, **1088**, 11–24.
- Takeuchi,R., Oshige,M., Uchida,M., Ishikawa,G., Takata,K., Shimanouchi,K., Kanai,Y., Ruike,T., Morioka,H. and Sakaguchi,K. (2004) Purification of Drosophila DNA polymerase zeta by REV1 protein-affinity chromatography. *Biochem. J.*, **382**, 535–543.
- Chen,H., Lawrence,C.B., Bryan,S.K. and Moses,R.E. (1990) Aphidicolin inhibits DNA polymerase II of Escherichia coli, an alpha-like DNA polymerase. *Nucleic Acids Res.*, **18**, 7185–7186.
- Pedrali-Noy,G. and Spadari,S. (1980) Mechanism of inhibition of herpes simplex virus and vaccinia virus DNA polymerases by aphidicolin, a highly specific inhibitor of DNA replication in eucaryotes. *J. Virol.*, **36**, 457–464.
- Frank,K.B., Derse,D.D., Bastow,K.F. and Cheng,Y.C. (1984) Novel interaction of aphidicolin with herpes simplex virus DNA polymerase and polymerase-associated exonuclease. *J. Biol. Chem.*, **259**, 13282–13286.
- Selwood,D.L., Challand,S.R., Champness,J.N., Gillam,J., Hibberd,D.K., Jandu,K.S., Lowe,D., Pether,M., Selway,J. and Trantor,G.E. (1993) Isosteres of the DNA polymerase inhibitor aphidicolin as potential antiviral agents against human herpes viruses. *J. Med. Chem.*, **36**, 3503–3510.
- Sheaff,R., Ilsley,D. and Kuchta,R. (1991) Mechanism of DNA polymerase alpha inhibition by aphidicolin. *Biochemistry*, **30**, 8590–8597.
- Sourlingas,T.G. and Sekeri-Pataryas,K.E. (1996) Aphidicolin large-scale synchronization of rapidly dividing cell monolayers and the analysis of total histone and histone variant biosynthesis during the S and G2 phases of the HEp-2 cell cycle. *Anal. Biochem.*, **234**, 104–107.
- Matherly,L.H., Schuetz,J.D., Westin,E. and Goldman,I.D. (1989) A method for the synchronization of cultured cells with aphidicolin: application to the large-scale synchronization of L1210 cells and the study of the cell cycle regulation of thymidylate synthase and dihydrofolate reductase. *Anal. Biochem.*, **182**, 338–345.
- Yagura,T., Kozu,T. and Seno,T. (1982) Arrest of chain growth of replicon-sized intermediates by aphidicolin during rat fibroblast cell chromosome replication. *Eur. J. Biochem.*, **123**, 15–21.
- Stephens,L., Hardin,J., Keller,R. and Wilt,F. (1986) The effects of aphidicolin on morphogenesis and differentiation in the sea urchin embryo. *Dev. Biol.*, **118**, 64–69.
- Pedrali-Noy,G., Belvedere,M., Crepaldi,T., Focher,F. and Spadari,S. (1982) Inhibition of DNA replication and growth of several human and murine neoplastic cells by aphidicolin without detectable effect upon synthesis of immunoglobulins and HLA antigens. *Cancer Res.*, **42**, 3810–3813.
- Cinatl,J. Jr, Cinatl,J., Kotchetkov,R., Driever,P.H., Bertels,S., Siems,K., Jas,G., Bindseil,K., Rabenau,H.F., Pouckova,P. et al. (1999) Aphidicolin glycinate inhibits human neuroblastoma cell growth in vivo. *Oncol. Rep.*, **6**, 563–568.
- Sessa,C., Zucchetti,M., Davoli,E., Califano,R., Cavalli,F., Frustaci,S., Gumbrell,L., Sulkes,A., Winograd,B. and D'Incalci,M. (1991) Phase I and clinical pharmacological evaluation of aphidicolin glycinate. *J. Natl Cancer Inst.*, **83**, 1160–1164.
- Edelson,R.E., Gorycki,P.D. and MacDonald,T.L. (1990) The mechanism of aphidicolin bioactivation by rat liver in vitro systems. *Xenobiotica*, **20**, 273–287.
- Arabshahi,L., Brown,N., Khan,N. and Wright,G. (1988) Inhibition of DNA polymerase alpha by aphidicolin derivatives. *Nucleic Acids Res.*, **16**, 5107–5113.
- Prasad,G., Edelson,R.A., Gorycki,P.D. and Macdonald,T.L. (1989) Structure-activity relationships for the inhibition of DNA polymerase alpha by aphidicolin derivatives. *Nucleic Acids Res.*, **17**, 6339–6348.
- Zhang,Y., Baranovskiy,A.G., Tahirov,T.H. and Pavlov,Y.I. (2014) The C-terminal domain of the DNA polymerase catalytic subunit regulates the primase and polymerase activities of the human DNA

- polymerase alpha-primase complex. *J. Biol. Chem.*, **289**, 22021–22034.
38. Minor,W., Cymborowski,M., Otwinowski,Z. and Chruszcz,M. (2006) HKL-3000: the integration of data reduction and structure solution—from diffraction images to an initial model in minutes. *Acta Crystallogr. D Biol. Crystallogr.*, **62**, 859–866.
 39. Brunger,A.T., Adams,P.D., Clore,G.M., DeLano,W.L., Gros,P., Grosse-Kunstleve,R.W., Jiang,J.S., Kuszewski,J., Nilges,M., Pannu,N.S. *et al.* (1998) Crystallography & NMR system: a new software suite for macromolecular structure determination. *Acta Crystallogr. D Biol. Crystallogr.*, **54**, 905–921.
 40. Krokan,H., Wist,E. and Krokan,R.H. (1981) Aphidicolin inhibits DNA synthesis by DNA polymerase alpha and isolated nuclei by a similar mechanism. *Nucleic Acids Res.*, **9**, 4709–4719.
 41. Wang,J., Sattar,A.K., Wang,C.C., Karam,J.D., Konigsberg,W.H. and Steitz,T.A. (1997) Crystal structure of a pol alpha family replication DNA polymerase from bacteriophage RB69. *Cell*, **89**, 1087–1099.
 42. Hiranuma,S., Shimizu,T., Yoshioka,H., Ono,K., Nakane,H. and Takahashi,T. (1987) Chemical modification of aphidicolin and the inhibitory effects of its derivatives on DNA polymerase alpha in vitro. *Chem. Pharm. Bull. (Tokyo)*, **35**, 1641–1644.
 43. Haraguchi,T., Oguro,M., Nagano,H., Ichihara,A. and Sakamura,S. (1983) Specific inhibitors of eukaryotic DNA synthesis and DNA polymerase alpha, 3-deoxyaphidicolin and aphidicolin-17-monoacetate. *Nucleic Acids Res.*, **11**, 1197–1209.
 44. Damia,G., Tagliabue,G., Zucchetti,M., Davoli,E., Sessa,C., Cavalli,F. and D'Incalci,M. (1992) Activity of aphidicolin glycinate alone or in combination with cisplatin in a murine ovarian tumor resistant to cisplatin. *Cancer Chemother. Pharmacol.*, **30**, 459–464.
 45. O'Dwyer,P.J., Moyer,J.D., Suffness,M., Harrison,S.D. Jr, Cysyk,R., Hamilton,T.C. and Plowman,J. (1994) Antitumor activity and biochemical effects of aphidicolin glycinate (NSC 303812) alone and in combination with cisplatin in vivo. *Cancer Res.*, **54**, 724–729.